662 ktv 伽瑪射線在康普吞攝像測量的可用性

張秋男・陳慶日・陳宏榮・黃福坤・游政陸

662 ktv 伽瑪射線對矽及鍺單晶的三個方向＜100＞、＜110＞及＜111＞的背角散射能譜由純鍺低能量偵測器測得，並利用傅立葉轉換的技術將之還原而得到矽與鍺單晶在＜100＞、＜110＞及＜111＞方向的康普吞攝像。此結果與由低能量光子或正子消滅等方法所得結果相比較，發現以相對論爲基礎得到的康普吞攝像是個定義清楚的概念，而用作康普吞攝像的 γ 射線高達 662 KeV 仍然適用。故銫 137 放射源可用作康普吞攝像的伽瑪射線源。

THE APPLICABILITY OF 662 KEV γ-RAYS TO COMPTON PROFILE MEASUREMENTS*

by

Chu-Nan Chang, Ching-Iue Chen, Hong-Zong Chen, Fu-Kwun Hwang and Jean-Luh You

Abstract

The 662 Kev γ-ray backscattered spectra of ‹100›-, ‹110›-and ‹111›-oriented Si and Ge were obtained by a HpGe low-energy detector. These spectra were then deconvoluted by a Fourier transformation technique. Compton profiles of ‹100›-, ‹110›- and ‹111›-oriented Si and Ge were deduced and compared with the existing data, which were obtained either by the method of lowenergy photons or by positron annihilation. The agreements are quite good, and we conclude that the Compton profile is a well defined concept in relativistic theory and is applicable to γ-ray energy as high as 662 KeV. Cs^{137} can thus be considered as a good radioactive source for Compton Profile measurements. We have also found that the multiple scattering effect at this photon energy is more significant for Si than for Ge.

Supported in part by National Science Council of R. O. C. under the grant No. NSC 74-0208 -M003-09.

I. Introduction

It is well known that based upon the impulse approximation(I.A.), the Compton backscattered spectrum can be used to profile the electron momentum distribution of a substance.[1,2] Both the non-relativistic and the relativistic I.A. give the following relation,[3,4,5]

$$\frac{d^2\sigma}{d\omega_2\, d\Omega} = C(\omega_1, \omega_2, \theta, p_z)\, J(p_z) \qquad (1)$$

In which the compton profile $J(p_z)$ can be factored out from the measurable double differential cross section $d^2\sigma / d\omega_2 d\Omega$ where $\hbar\omega_1$ and $\hbar\omega_2$ are respectively the energies of the incident and the scatterd photons, θ is the scattering angle, and p_z is the electron momentum projected in the direction of $z = \vec{k}_1 - \vec{k}_2 / |\vec{k}_1 - \vec{k}_2|$ ($\vec{k}_1$ and $\vec{k}_2$ are the momentum vectors of the incident and the scattered photons respectively). $J(p_z)$ is called the Compton profile and is actually the electron momentum distribution of P_z. $J(p_z)$ can thus be written as $J(p_z) = \int_{p_z} N(\vec{P})\, dp_x dp_y$, where $N(\vec{P})$ is the distribution of the electron momentum $\vec{p}$.

The factor $C(\omega_1, \omega_2, \theta, p_z)$ in equation (1) is theoretically calculable, either relativistically or non-relativistically, Fig.1 shows the results calculated by the methods of non-rel. and rel.I.A.. Both of them are normalized at $\hbar\omega_2 = 148.05$ Kev for this study.

The Compton-profile technique has been devloped and used for the past 30 years or so with X-rays as the photon source, and has made considerable contributions in the study of the electronic structure of atoms[6, 7, 8, 9]. But the measurements have been restricted to substances with low photoelectric absorption at X-rays energies used. Recent work has shown that this restriction is no longer necessary when a high-energy γ-ray source is used in conjunction with a high resolution semiconductor detector.[1, 10]

Typical γ-ray sources in use are Am ^{241} (59.54Kev) and Te ^{123m} (159.0kev), but sources with considerably higher energies are currently under consideration. A serious complication of the γ-ray technique is, however, that the energy transfers are so large that relativistic effects must be considered. This will in general lead to question as to whether Compton-profile is still a well-defined concept or not. Fortunately, this problem has been investigated and shown theoretically that wirhin the limit of impulse approximation, the Compton profile is still a well-defined and useful concept. [4,5]

The proposed theory of relativistic Compton profile has been tested experimentally for just a few cases. [11, 12] In this paper, we will report the results obtained by using Cs ^{137} (662Kev) as a γ-ray source, a promising r-ray source for future Compton profile measurements, to measure the Compton profile of Si and Ge which have long been measured and investigated by X-ray scattering[8] and positron annihilation techniques.[13] The high energy γ-ray relativistic effect proposed by the theory can be verified additionally through the comparison of the Compton profile of γ-rays with those of X-rays and positron annihilation. This would provide an additional proof for the validity of the concept of Compton provile at high-energy γ-rays.

II. Experimental

The whole arrangement of the experimental set-up is sketched in Fig. 2. The γ-ray source, Cs 137, of about 1.2 Ci is housed in a lead cylinder that serves as a collimator and a radiation shield. the detailed structure of this source house was described in Ref.14. The target chamber was kept at a high vacuum of about 10^{-5} torr to eliminate the background cotribution by air scattering. Two beryllium

windows of 0.254 mm thick were placed in the chamber to transmit the incident beam and to transmit the scattered beam to a HpGe detector at a scattering angle of 155. The chamber length is 38 cm in order to eliminate as much as possible the backscattering from the chamber.

By using an X-ray film in place of the target, the size of the beam of the target was measured to be circular in shape and was 1.2 cm in diameter.

The HpGe detector is well shielded with lead. The background with the beam on is shown in Fig. 3, which shows that the background is quite low in the region of 150 KeV where the profile spectrum is to be located. Fig.4 and Fig. 5 show respectively the typical spectra obtained from ‹110›-oriented Ge and Si single crystals. Lead K X-rays detected at the low-energy side of the spectrum probably came from the lead shielding around the detector. The origin of the 59.4 Kev peak was found to be a result of the contamination of our shielding brick with trace amount of Am^{241}. Both the 59.4 Kev γ-ray and the lead K X-rays were used to check the stability of our data acquisition system during a single run which usually lasted for 10 hours.

Prior to add up all the runs together to form a finall spectrum, the energy scale of each run was examined and rescaled if necessary. Usually, more than 10 runs are necessary to reach a good statistics of about 2.5%

The solid angle at the detector was so arranged that the dispersion of the scattering angle $\Delta\theta$, determined geometrically, was less than 1.0 degree which corresponds to an energy dispersion of $\Delta E \simeq 640$eV, which is within the resolution ($\simeq$720 eV) of the detector at the photon energy of 192 KeV.

Both Si and Ge targets are single crystals oriented in the directions of ‹111›, ‹110› and ‹100› and are in the form of thin wafers with a thickness of 5mm and a diameter of 2.5cm.

The total counting rate was about 10 counts/min. The signal to noise ratio was about 15:1.

A Th^{232} source was used to determine the resolution function, of the detector,and Fig.6 shows the 238.6 KeV peak where the solid line was the raw spectrum, and the dotted line was deduced from the raw data by letting the low-energy tail stripped off. This is accomplished by subtracting from each data point an amount proportional to all counts measured at higher energies. For a constant tail, this can be expressed as,

$$R'(W) = R(W)-C_1\int_W^{W_1} R'(W)dw \qquad (2)$$

where $R'(W)$ is the effective resolution function, W_1 is the high energy bound of the spectrum, and C_1 is an adjustable constant.

Since the peak energy of the Compton spectrum was 192 KeV, the resolution function to be used in deconvolution must be scaled down from the effective resolution shown in Fig. 6 for 238.6 KeV. It is found that the resolution function is very nearly gaussian and the resolution ΔE is very closely proportional to $\sqrt{E}$, so that the resolution function we have finally used is a gaussian function with a width of ΔE=720 eV.

III. Data regression.

Since the real spectrum is convoluted by the instrumentation function. to obtain the real spectrum, a deconvolution technique must be applied to the raw spectrum such that the real double differential cross section $\frac{d^2\sigma}{d\Omega d\omega_2}$ and hence the Compton-profile J(Pz) can be deduced. Fourier analysis technique of deconvolution is used in our analysis.

The Compton backscattered spectrum $F(\omega_2)$ is the spectrum obtained at a HpGe γ-ray detector (with about 3% of resolution), but having the background subtracted, the detector's efficiency corrected and the low energy tail stripped off. Typtical spectra for <110>-oriented Ge and Si are shown

in FIg. 7 and Fig. 8 respectivly. The total channels used for analyzing the spectrum is 2048, and the total channels of the $F(\omega_2)$ spectrum to be deconvoluted is 700. The intrumentation function $G(\omega)$ used in deconvolution is the combination of the resolution function of the detector and the geometrical dispersion function. The resolution function of the detector has been described in the last section. The geometrical dispersion function was obtained through a computer simulation program, by assuming that the incident beam on the target was uniformally distributed in the area covered by the beam size. This is shown in Fig. 9, which looks very much like a triangle.

The desired profile spectrum $f(\omega_2)$ can be deconvoluted from the following convoluted equation,

$F(\omega_2) = \int_{-\infty}^{\infty} f(\omega)G(\omega_2-\omega)d\omega$ as $F(K)=f(K)*G(K)$, where the functions of K are the Fourier transforms of the corresponding functions of ω.

The deconvolution spectrum f(W2), transferred from f(K) with K cut off at different values, were searched. We found that K=65 is the optimum value. Typtical deconvoluted spectra as well as their original spectra for ‹100› , -‹110›- and ‹111›-, oriented Si and Ge targets are shown respectively in Fig. 10 and Fig. 11 with the high-energy cut-off selected at 201 KeV. Above 201 KeV, the statistics is too poor to obtain meaningful data.

According to equation (1), the deconvolution spectrum divided by the factor $C(\omega_1, \omega_2, \theta, p_z)$ which can be calculated from the rel. I. A. theroy, is the Compton-profile $J(P_z)$. As can be seen from Fig. 7 and 8, the backscattering of the photons by the chamber wall inevitably contributes to the left end of the profile spectrum. Considering the experimental geometry, the energy of the photons was estimated to be 184 KeV, while the peak energy of the profile spectrum is about 192 KeV. As a result, the spectrum becomes asymmetrical about the central peak. However, the right side of the profile spectrum is not contaminated, and was used to obtain J(Pz). J(Pz) was normalized as $\int_0^{p_z} J(p_z)\,dp_z = N/2 - \int_{p_z}^{\infty} J(p_z)dp_z$,

where N is the total number of electrons around the scattering atom, i.e. the area under the profile curve was normalized to one half of the total number of electrons per atom minus the impulse-approximation contributions of the inner-core electrons (Pz=7a.u. for Si and 6a.u. for Ge). The $j(P_z)$ of the inner-core eelectrons was taken as the theoretical values given by F. Biggs et al.[16] The peak position corresponding to Pz=o was chosen at the peak of the profile spectrum. The results are shown in Fig. 12 and Fig. 13 for <100>-<110>-and <111>- oriented Si and Ge respectielỷ, but no multiple scattering correction was taken into account in the deduction of these data.

IV. Results and discussion

The Compton-profile data we have obtained for the valence electrons of Si and Ge in three scattering directions are listed in table 1 and table 2 respectively. Included in these tables are various theoretical values and experimental data by others for comparison. Reed and Eisenberger's results[10] are shown, along with our data in Fig. 12 and Fig. 13 for comparisons. We have found that the agreement between these two sets of experimental results is reasonably good within the statistic errors for Ge. But for Si, our data sysmetically shows a small deviation from those of Read and Eisenberger. This seems to indicate that at the γ-ray energy of 662 Kev, the multiple-scattering effect for 5mm Ge is somewhat negligble, but it is sizable for 5mm Si. We will investigate this effect in the future by using different thickness of Ge and Si as targets for Compton profile measurements and by making a Monte Carlo calculation[19].

We have also used the non-relativistic $C(\omega_1, \omega_2, \theta, p_z)$ factor to deduce the Compton-profiles of Si and Ge in the directions of <111>, <110> and <100>, and found the results deviating substantially from the existing data. Thus we

conclude that γ-rays of 662 KeV can be used for Compton profile measurements, and that the rel. I.A. theory can be applied to the analysis of the Compton-profile. The Compton profile measurement of the substances across the whole periodic table is no longer limited by the large photoelectric absorption cross-section [17, 18], and can be done with the long-lived stable and somewhat inexpensive γ-ray (662 KeV) source of Cs^{137}.

Figure Captions

Fig. 1 The $C(\omega_1, \omega_2, \theta, p_z)$ for rel. I.A. (C_R) and non-rel. I.A. (C_{NR})

Fig. 2 Schematic diagram of experimental arrangemt

Fig. 3 The background with photon beam on

Fig. 4 The whole r-ray backscattering spectrum of <110>-oriented Ge

Fig. 5 The whole r-ray backscattering spectrum of <110>-oriented Si

Fig. 6 The 238.6KeV spectrum of Th^{232}

Fig. 7 The Cpmpton spectrum of <110>-Ge with the background subtracted and the low enery tail stripped off (dot). The orignal spectrum (solid) is also shown for comparison,

Fig. 8. The COmpton spectrum of <110>-Si with the background subtracted and the low-energy tail stripped off (dot). The original spectrum (solid) is also shown for comparison.

Fig. 9 The geometrical resolution function of our experimental set-up

Fig. 10 The deconvoluted spectra (dot) as well as the original spectra (solid) for<100>-, <110>- and <111>-oriented Si.

Fig. 11 Same as in Fig.11, but for Ge.

FIg. 12 The Compton profiles of Si with scattering direction along the <100>, <110> and <111> directions (solid). Data from Ref. 10(dot) are also included for comparison.

Fig. 13 Same as in Fig. 12, but for Ge.

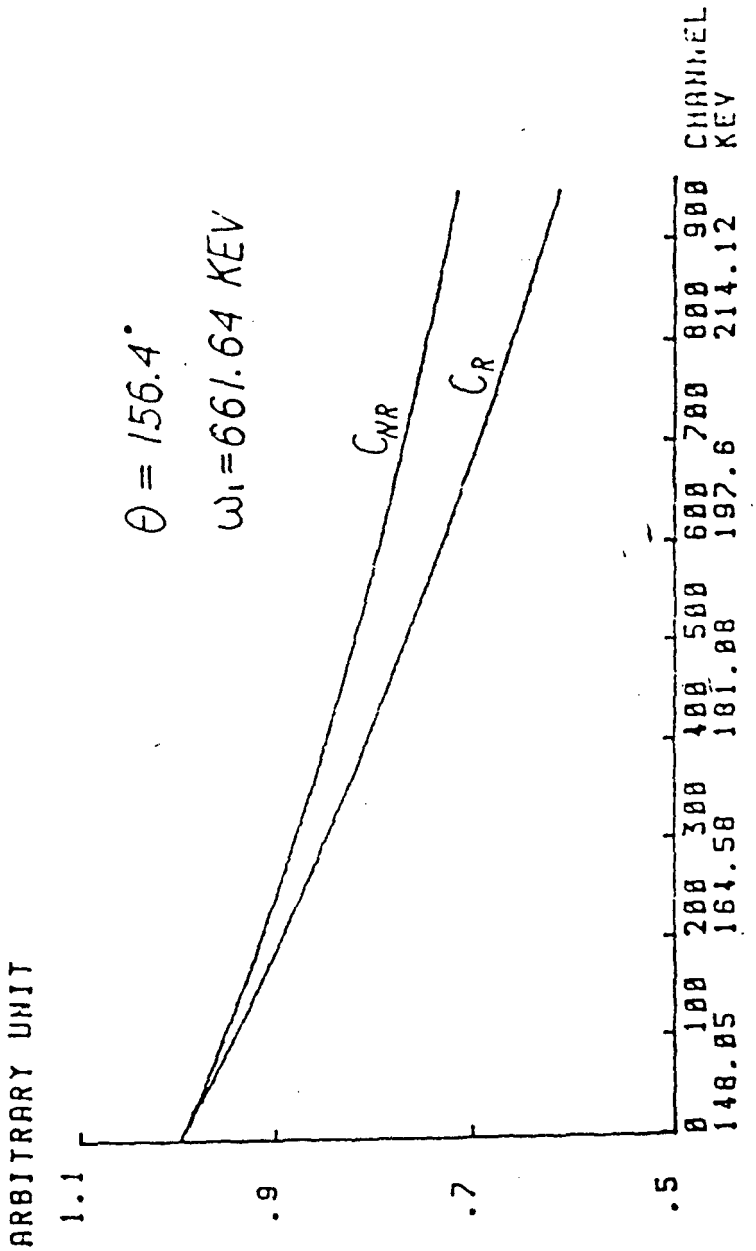

Fig. 1 The C(ω_1, ω_2, θ, p_z) for rel. I.A. (C_R) and non-rel. I.A. (C_{NR})

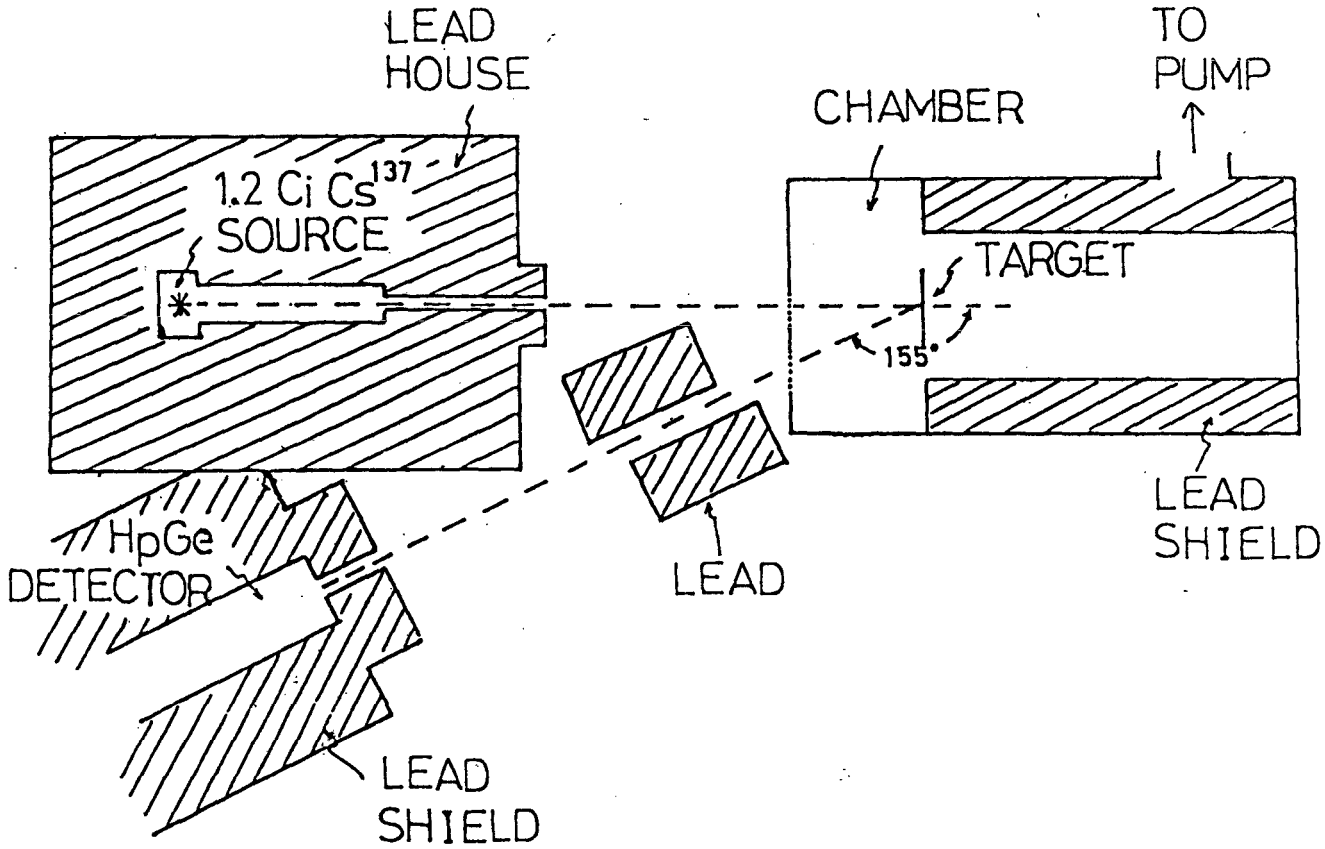

Fig. 2 Schematic diagram of experimental arrangement

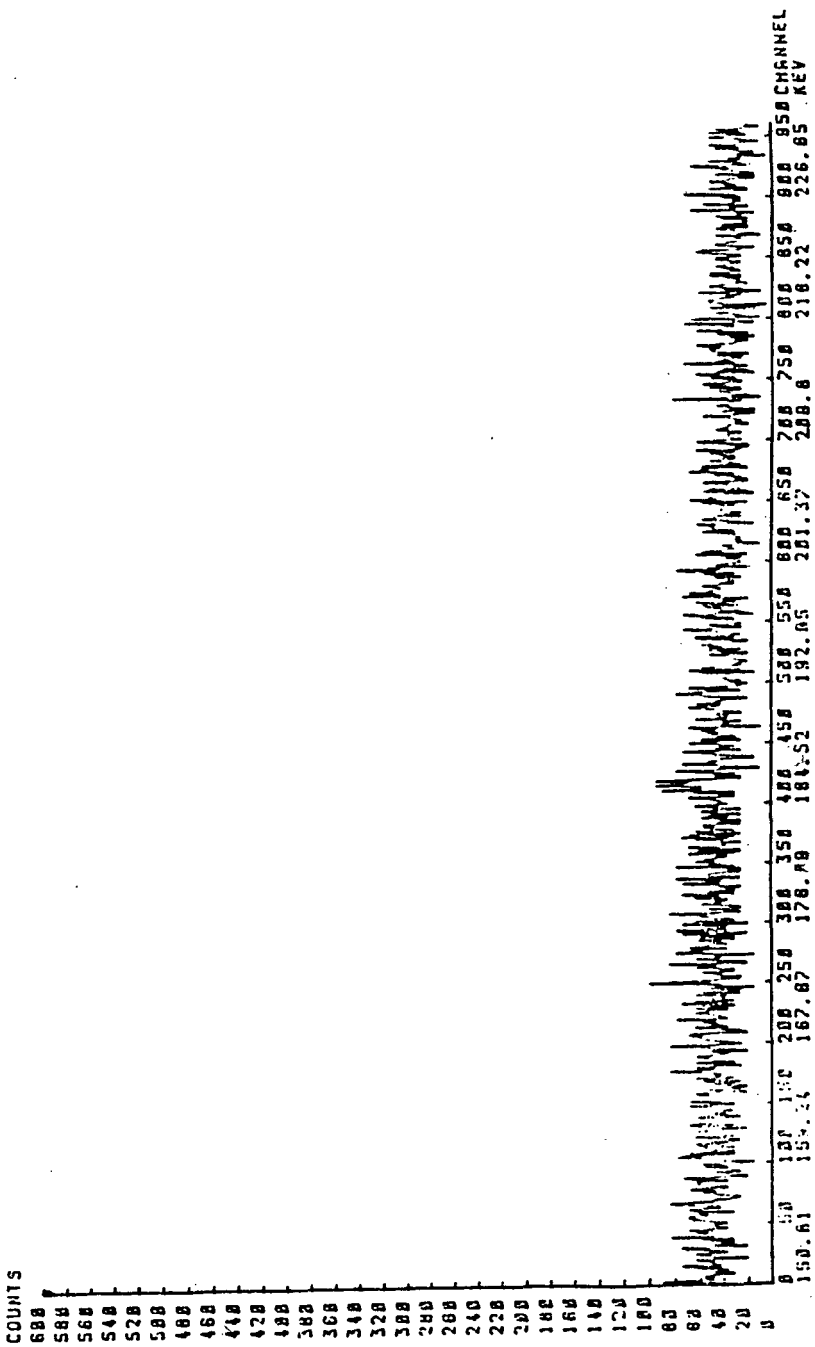

Fig. 3 The background with photon beam on

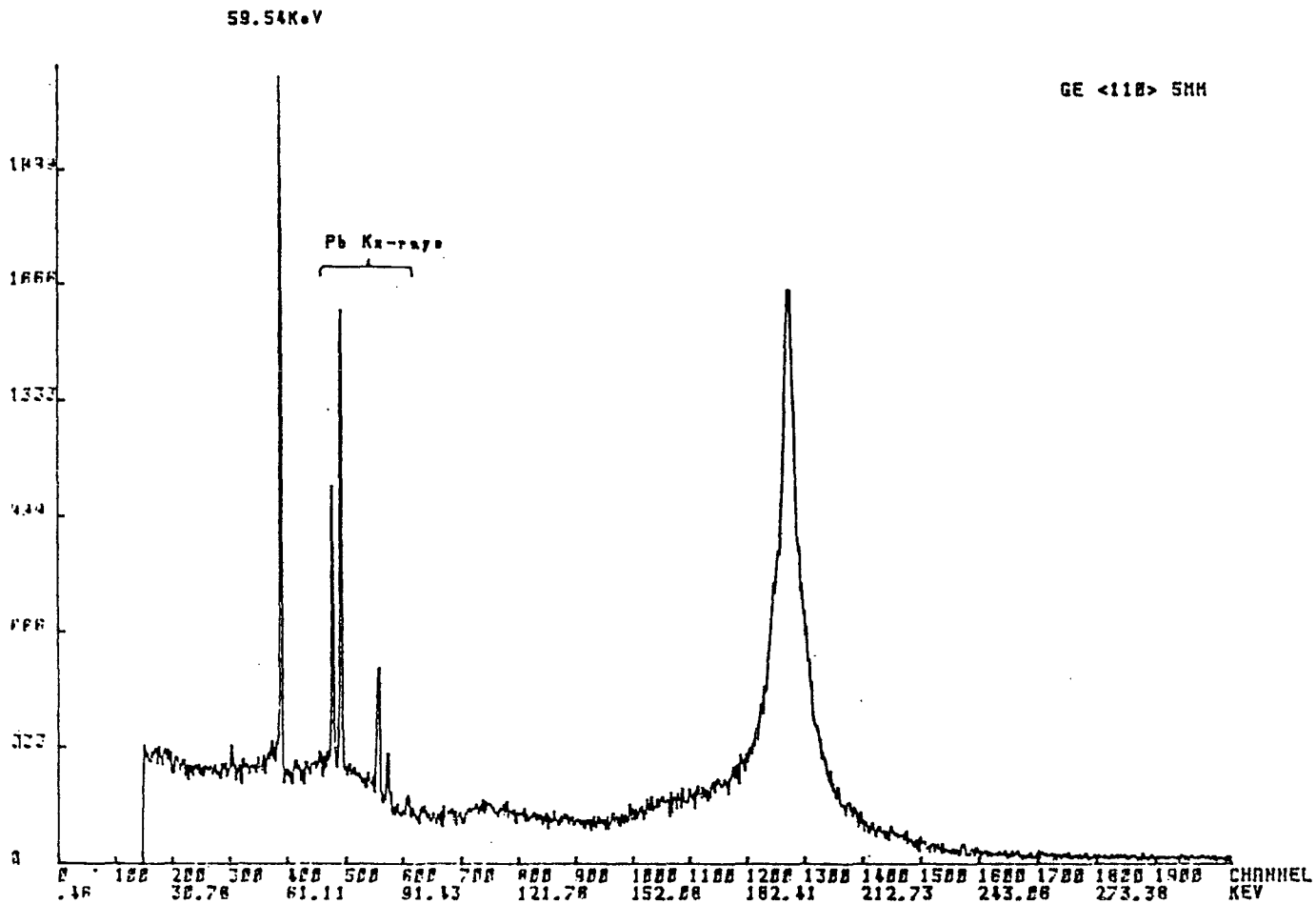

Fig. 4 The whole γ-ray backscattering spectrum of <110>-oriented Ge

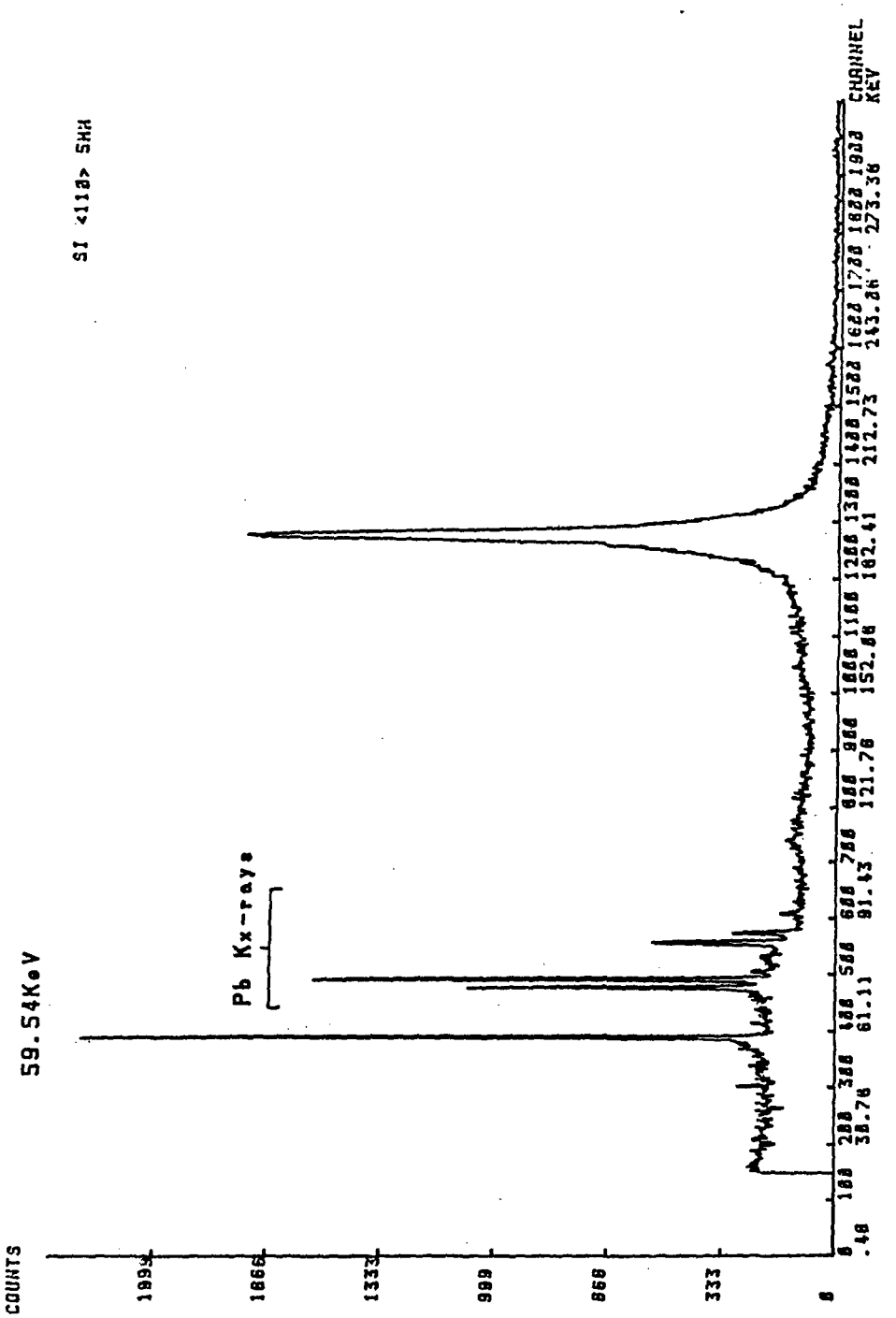

Fig. 5 The whole γ-ray backscattering spectrum of <110>-oriented Si

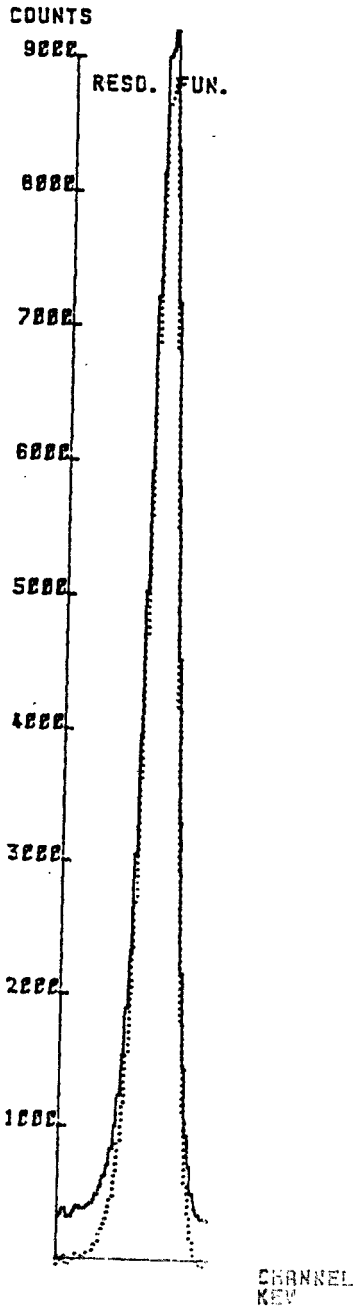

Fig. 6 The 238 (KeV) spectrum of Th^{232}

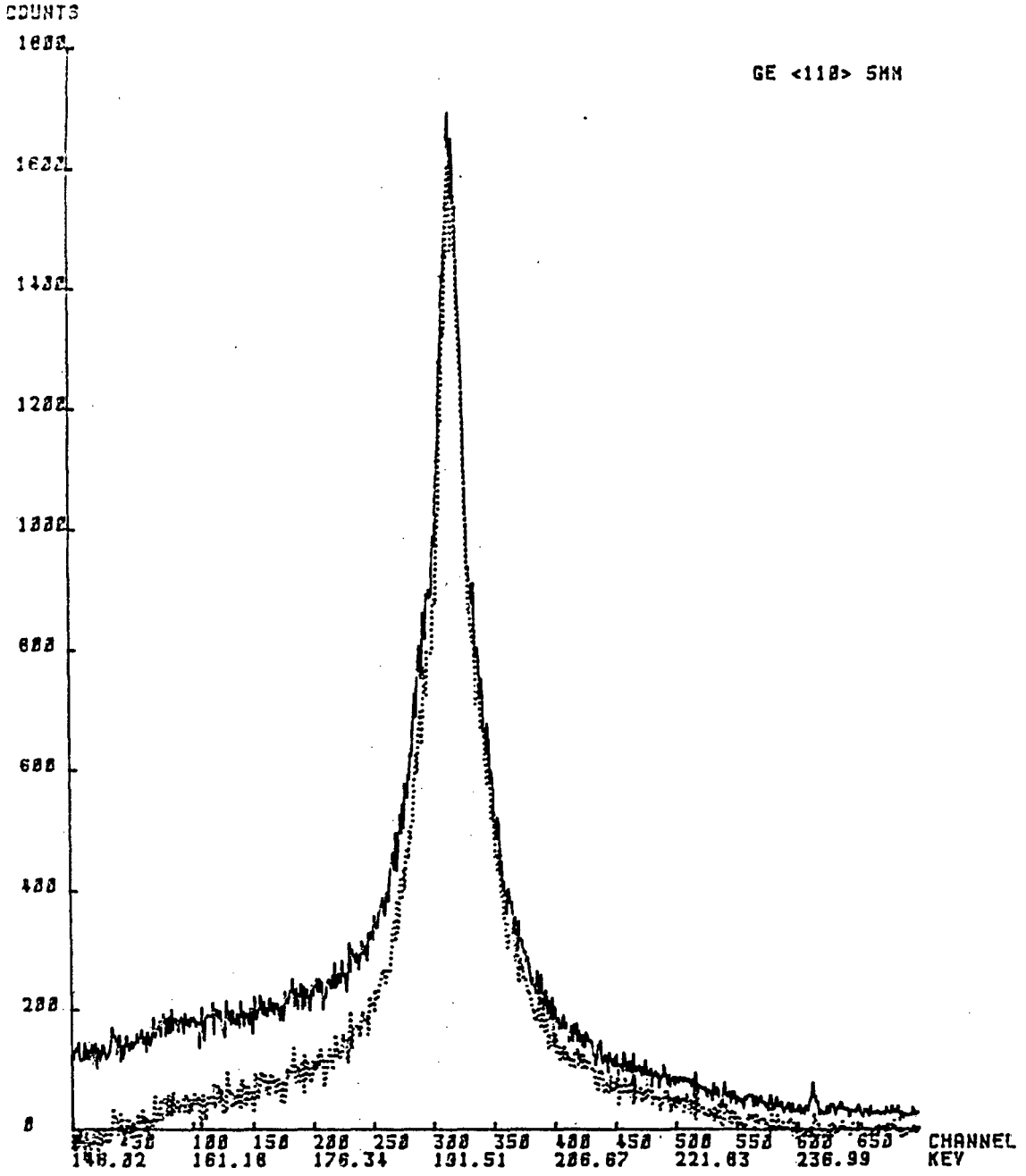

Fig. 7 The Compton Spectrum of <110>-Ge with the background subtracted and the low energy tail stripped off (dot). The original spectrum (solid) is also shown for comparison.

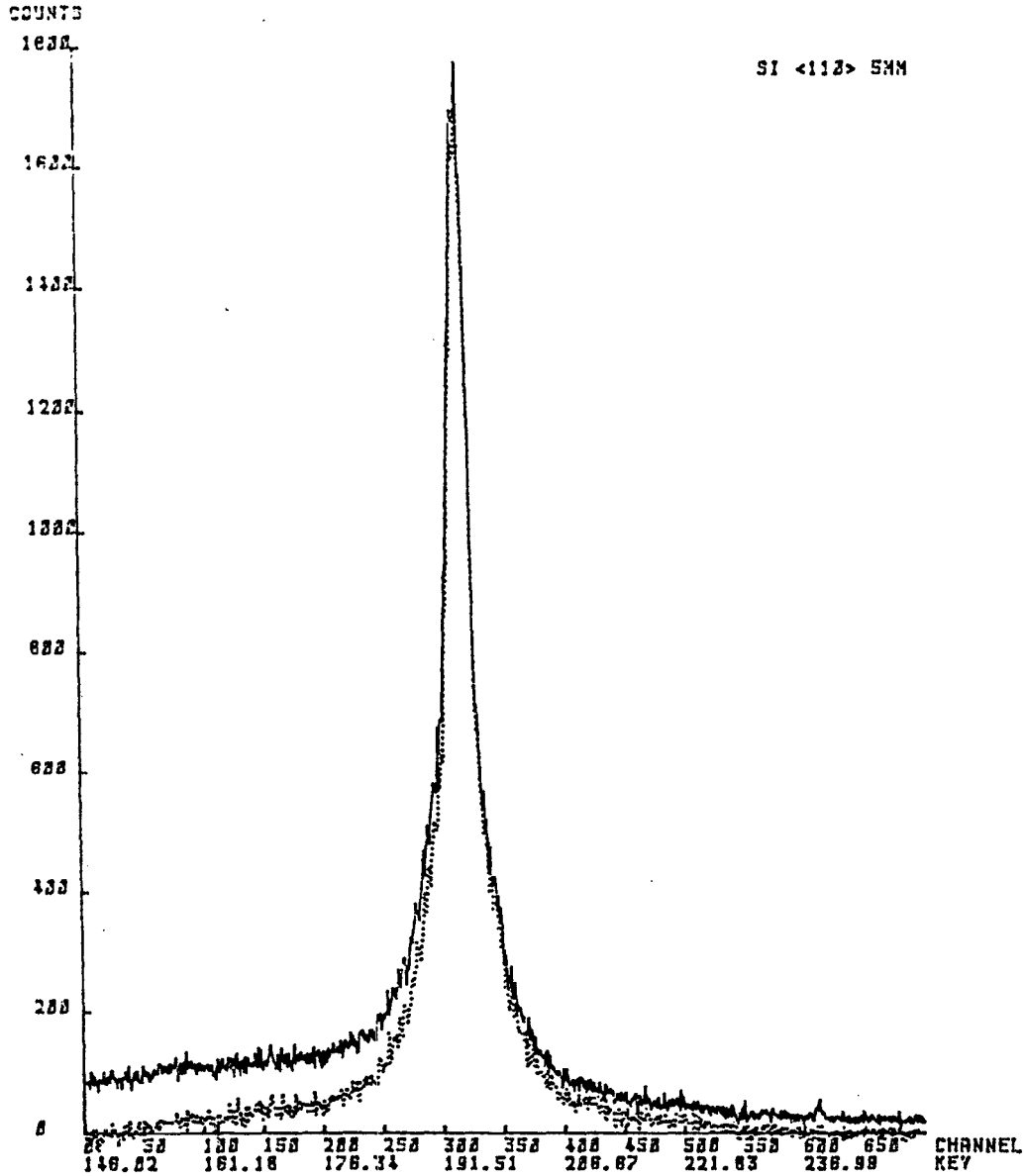

Fig. 8 The compton spectrum of <110>-Si with the background subtracted and the low-energy tail stripped off (dot). The original spectrum (solid) is also shown for comparison.

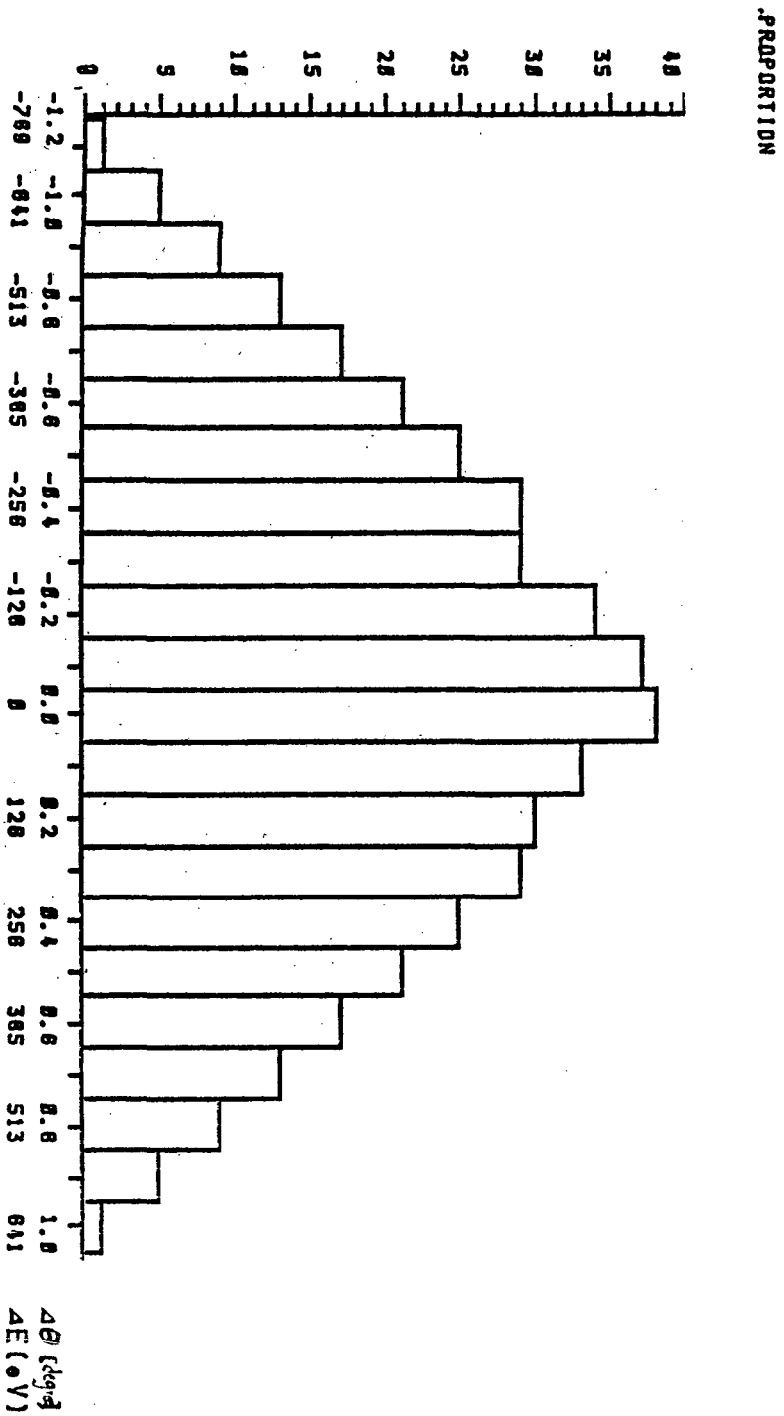

Fig. 9 The geometrical resolution function of our experimental set-up

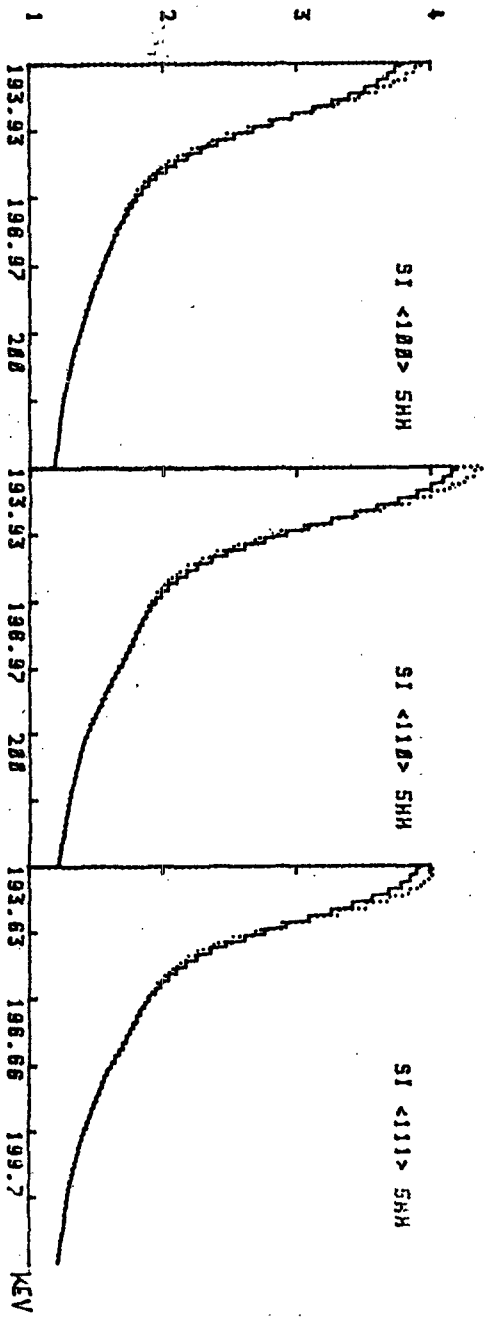

Fig. 10 The deconvoluted spectra (dot) as well as the original spectra (solid) for <100>-, <110>- and <111>- oriented Si.

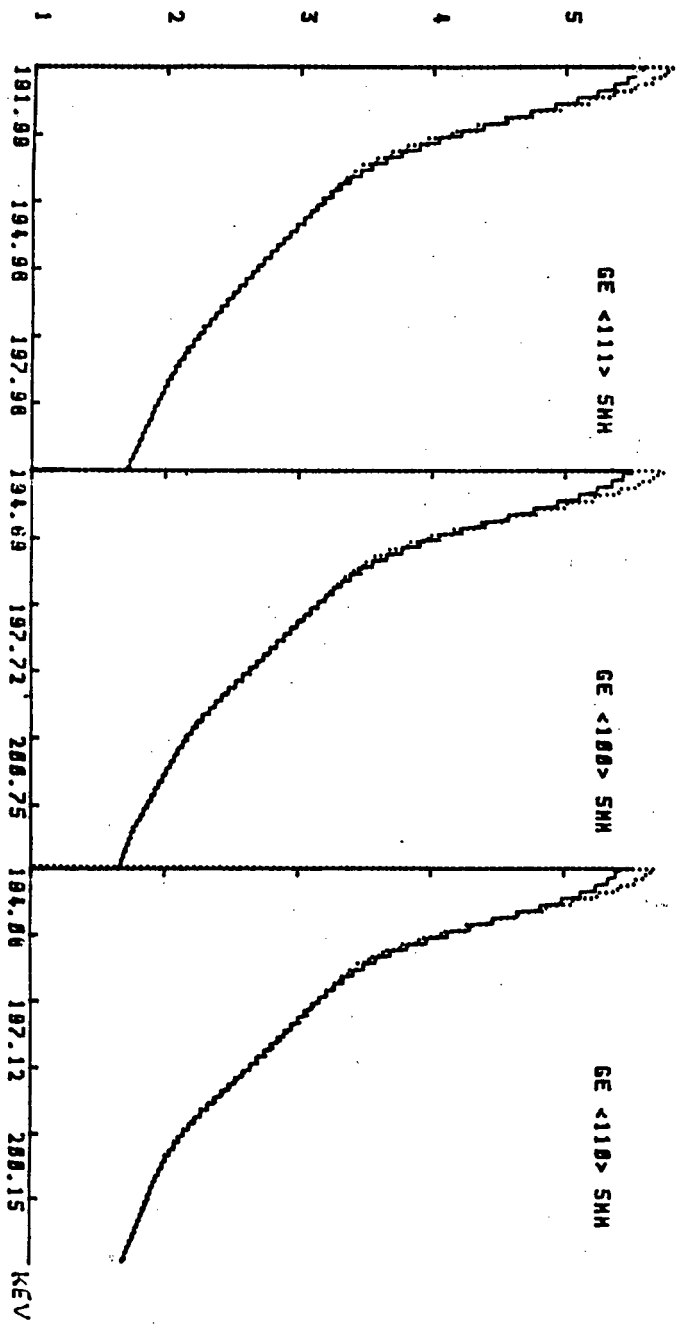

Fig. 11 Same as in Fig.11, but for Ge

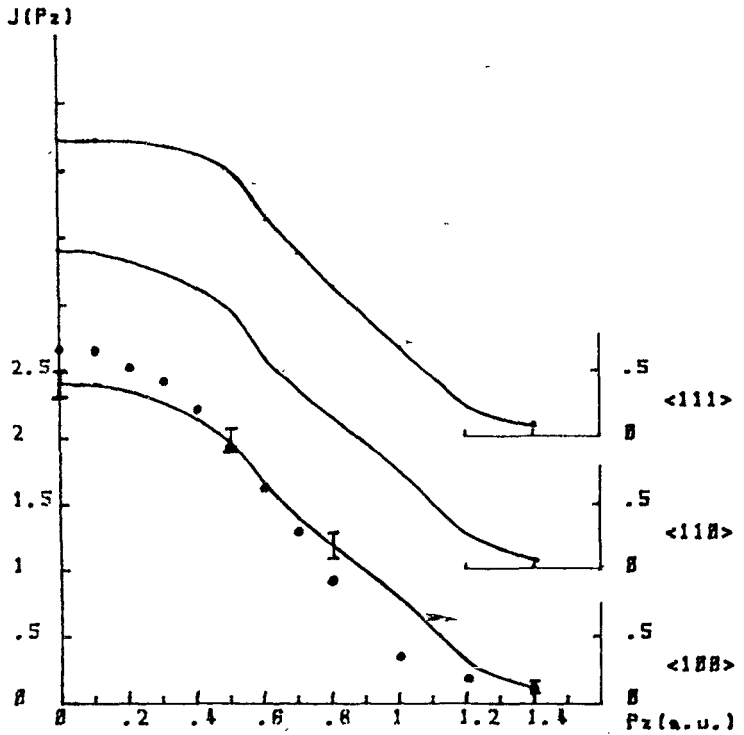

Fig. 12 The compton profiles of Si with scattering direction along the <100>, <110> and <111> directions (solid). Data from Ref. 10(dot) are also included for comparison.

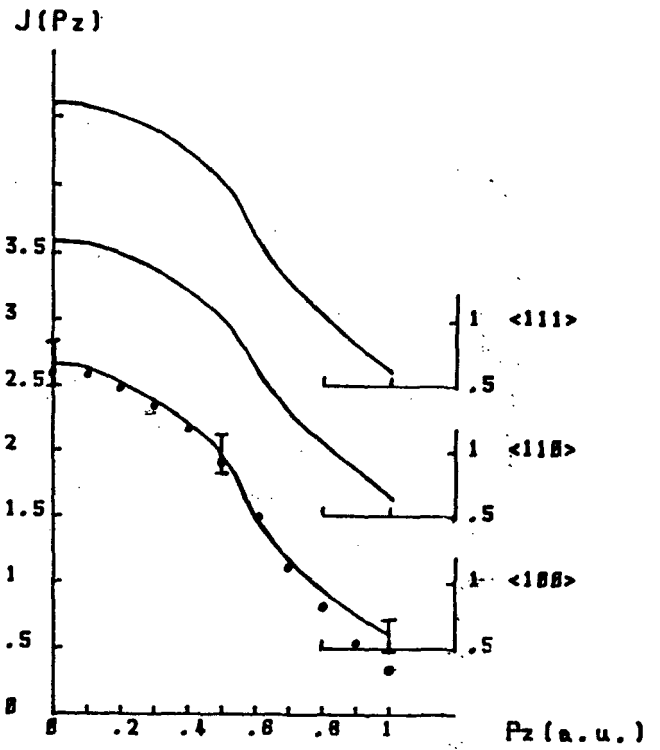

Fig. 13 Same as in Fig. 12, but for Ge

References

1. B. Williams, ed. "Compton Scattering: The Investigation of Electron moMentum Distributions" McGraw-Hill, New York (1977).
2. M. J. Cooper, Contemp. Phys., Vol. 18, No.5, pp.489-517 (1977).
3. P. Eisenberger and W. A. Reed, Phys. Rev. A5, 2085 (1972) R. Currat, P.D. Decicco and R. J. Weiss, Phys. Rev. B4 No.12,4256 (1971).
4. P. Eisenberger and W. A. Reed, Phys. Rev. B9, No. 8, 3237-3241 (1974).
5. Roland Ribberfors, Phys. Rev. B12, 2067(1975) and Phys. Rev.B12, 3136 (1975)
6. W.C. Phillips and R. J. Weiss, Phys, Rev. 171, No.3, 790(1968).
7. P. Eisenberger, Phys. Rev. A2, No.5, 1678(1970).
8. R.J. Weiss, Phil. Mag. 26, 153(1972).
9. W. Schulke, Phys. Stat. Sol. (b) 62,453 (1974).
10. W. A. Reed and P. Eisenberger, Phys. Rev. B6, No.12, 4596 (1972)
11. M. Cooper, P. Pattison and J. R. Schneider, Phill, Mag. Vol.34 No.2 243-257 (1976).
12. J.L. DuBard, Phill. Mag. B37, No.3, 273-283 (1978).
13. D. Stroud and H. Enreneich, Phys. Rev. 171, No.2, 399-407 (1966).
14. C. N. Chang, C.c. Kuo and C. I, Chen, Proc. of Nat'l Sci. Council, Taiwan, R.O.C., Part B, Vol.5, No.2, 125-133(1981).
15. T. Ihouye, Nucl. Instr. and Meth.67, 125-132 (1969) and P. Paatero, S. Manninen and T. Paakkari, Phil. Mag. 32, 1281-1294 (1974).
16. F. Biggs, L.B. Mendelsohn and J.B. Mann, Atomic Data and Nuclear Data Table 16, 201-309 (1975).
17. J. L. DuBard, Sci. Instrum., Vol.12, 302-307 (1979).

18. G. Angonoa, R. Dovesi, C. Pisani and C. Roetti, Phil. Mag. B44, No.3, 413-418 (1981).
19. J. Felsteiner, P. Pattison and M. Cooper, Philos, Mag. 30 527-548 (1974) and J. Felsteiner and P. Pattison, Phys. Rev. B13 No.6, 2702-2704 (1976).
20. W. SLHULKE and W. LUCHT, Phys. stat sol. (b) 59 K107 (1973).
21. V.V. Bhokare and R.M.Sinhtu, Phys. stat. sol. (b) K161-K163(1976).

Table 1. The Compton profiles of Si valence electrons for the <100>, <110> and <111> directions

P_z	Core a) $1S^2\ 2S^2\ 2P^6$	This work				Other's experimental work						Theoretical values			
		<100>	<110>	<111>	average	b) Positrons	X-rays	c) <100>	d) <100>	d) <110>	d) <111>	a) Free Atom	e) Free Atom	e) Free electron	e) Band Theory
0.0	1.571	2.42 ±0.10	2.40 ±0.09	2.22 ±0.09	2.35	2.64	2.54	2.569 ±0.01	2.81	2.83	2.75	3.56	3.54	3.13	2.58
0.1	1.569	2.42	2.40	2.23	2.35	2.63	2.52	2.567	2.75	2.78	2.70	3.47	3.45	3.10	2.56
0.2	1.565	2.36	2.33	2.22	2.30	2.57	2.46	2.543	2.62	2.65	2.59	3.20	3.18	3.00	2.51
0.3	1.557	2.27	2.24	2.18	2.23	2.44	2.30	2.444	2.47	2.47	2.46	2.77	2.77	2.82	2.38
0.4	1.545	2.15	2.12	2.11	2.13	2.26	2.12	2.237	2.27	2.25	2.25	2.20	2.26	2.58	2.16
0.5	1.530	1.99 ±0.10	1.96 ±0.10	1.99 ±0.10	1.98	2.00	1.92	1.943	2.02	1.96	1.97	1.73	1.74	2.28	1.91
0.6	1.508	1.61	1.57	1.63	1.60	1.39	1.63	1.614	1.66	1.64	1.69	1.26	1.37	1.91	1.61
0.7	1.488	1.39	1.35	1.39	1.38	1.32	1.31	1.278	1.28	1.35	1.37	0.88	0.89	1.46	1.29
0.8	1.462	1.18 ±0.09	1.14 ±0.09	1.13 ±0.08	1.15	0.94	1.03	0.928	0.99	1.06	1.10	0.60	0.61	0.95	0.94
1.0	1.405	0.78	0.74	0.68	0.73	0.28	0.49	0.347 ±0.04	0.56	0.54	0.62	0.27	0.28	0.37	0.34
1.2	1.338	0.29	0.26	0.22	0.26	0.12	0.21	0.175	0.29	0.25	0.24	0.13	0.14	0.00	0.13
1.4	1.257	0.06	0.06	0.05	0.10	0.08	0.08	0.119	0.13	0.12	0.11	0.08	0.08		0.11

a) from Ref.16; b) averaged over the <100>, <110> and <111>, directions from Ref.8;
c) from Ref.10; d) from Ref.20; e) from Ref.8

Table 2. The Compton profiles of Ge valence electrons for<100> <110>and<111>

P_Z	a) Core $1S^2\ 2S^2\ 2P^6\ 3S^2\ 3P^6\ 3D^{10}$	This work				b) Other's experimental work<100>	c) Theoretical value (free atom)
		<100>	<110>	<111>	average		
0.0	3.432	2.65 ±0.15	2.56 ±0.15	2.58 ±0.15	2.60	2.581 ±0.02	3.598
0.1	3.434	2.64	2.55	2.57	2.59	2.577	3.506
0.2	3.426	2.54	2.47	2.49	2.50	2.509	3.234
0.3	3.410	2.40	2.36	2.38	2.38	2.376	2.800
0.4	3.396	2.21	2.20	2.22	2.21	2.168	2.264
0.5	3.380	1.98 ±0.15	2.00 ±0.14	2.02 ±0.14	2.00	1.874	1.720
0.6	3.366	1.44	1.53	1.54	1.50	1.497	1.234
0.7	3.340	1.16	1.27	1.28	1.24	1.118	0.850
0.8	3.302	0.93	1.05	1.04	1.01	0.805	0.568
1.0	3.230	0.51 ±0.12	0.60 ±0.12	0.60 ±0.12	0.57	0.305 ±0.07	0.250

a)from Ref.16

b)from Ref.10

c)from Ref.16. But the values obtained from a pseudopotential calculation[20] are much closer to the results of Ref.10 as our.